Stereocorrelation of Landsat TM Images

Manfred Ehlers and *R. Welch*
Laboratory for Remote Sensing and Mapping Science, Department of Geography, University of Georgia, Athens, GA 30602

ABSTRACT: A DEM developed from Landsat TM images of a rugged terrain area in north Georgia by automated stereocorrelation techniques yielded an $RMSE_z$ value of ± 42 m. Based on the *B/H* ratio of 0.18 for the Landsat data, this Z-error corresponds to a planimetric correlation accuracy of about ± 0.3 pixels, confirming that precise correlation can be achieved with operational satellite data. Contours at a 100–m interval interpolated from the DEM show a deviation of ± 33 m from reference contours obtained from existing 1.:24,000–scale maps. The 28.5–m pixel resolution and the weak *B/H* ratio impose limitations on the accuracy that can be achieved with Landsat TM data. However, it is anticipated that $RMSE_z$ values of ± 10 m or less can be achieved with SPOT–1 panchromatic stereo images of 10–m resolution recorded at *B/H* ratios of 0.5 to 1.0. DEMs generated by stereocorrelation techniques can be used to create orthoimages, perspective views, and topographic map products.

INTRODUCTION

IN RECENT YEARS digital image data recorded by mechanical scanners from stable satellite platforms have been rectified to a fraction of a pixel, demonstrating that planimetric accuracies compatible with map scales of 1:50,000 to 1:250,000 can be easily achieved (Wong, 1975; Bernstein, 1976; Welch and Usery, 1984; Borgeson, *et al.*, 1985). However, the possibilities for deriving terrain elevations (Z-coordinates) by automated stereocorrelation techniques from digital images have been limited by the absence of satellite stereo data recorded at reasonable base-to-height (*B/H*) ratios.

Theoretical studies undertaken in support of proposed mapping satellites such as Stereosat and Mapsat indicate that automated digital techniques can provide vertical accuracies of ± 0.3 to ± 1.0 pixel (Welch and Marko, 1981; Colvocoresses, 1982; Welch, 1983; Murai and Shibasaki, 1984). These accuracies have been confirmed in operational experiments conducted with Landsat multispectral scanner (MSS), return-beam vidicon (RBV), and thematic mapper (TM) data recorded from adjacent orbits, and with SPOT simulation image data (Simard and Krishna, 1983; Simard *et al.*, 1984; Welch and Ehlers, 1985; Rose *et al.*, 1986; Rosenholm, 1986).

Of course, if automatic correlation techniques are to be accepted for mapping applications, they must be proved reliable and provide a sufficient density of point elevations from which contours can be interpolated. In order to derive accurate terrain elevations from digital images by means of stereocorrelation, the images must be geometrically corrected for systematic distortions introduced during the recording process and rectified to the terrain coordinate system. When geometrically corrected data sets forming a stereopair are placed in register, the residual planimetric differences in the x-coordinates are assumed to result from relief displacement and can be determined to a fraction of a pixel by automatic correlation techniques. The differences in *x*-parallax may then be used in conjunction with a mathematical model based on the geometry of the stereo acquisition system to compute relative elevations or height differences. By referencing the relative elevations to a few control points with known Z-coordinates, absolute elevations can be determined and the accuracy of the procedure can be evaluated. Once an absolute digital elevation model (DEM) has been generated, it may be used to create contour maps and slope and aspect maps, or to produce relief-corrected orthoimages (Figure 1).

The objective of this paper is to describe a stereocorrelation software system, based on the above principles, that was developed by the Laboratory for Remote Sensing and Mapping Science (LRMS) for use with digital image data recorded in either the cross-track or along-track direction. It has proved reliable for obtaining *X*, *Y* and *Z* coordinates from Landsat TM data acquired from adjacent orbits and will be applied to SPOT High Resolution Visible (HRV) image data as part of a Programme d'Evaluation Preliminaire SPOT (PEPS) experiment.

DATA SETS AND STUDY AREA

Two adjacent Landsat–4 TM scenes corresponding to path 18, row 36 (P18R36) and path 19, row 36 (P19R36) in the Landsat–4/-5 Worldwide Reference System (WRS) were acquired in CCT-pt format from the National Aeronautic and Space Administration's (NASA) Goddard Space Flight Center during the Landsat Image Data Quality Analysis (LIDQA) program investigations (Welch *et al.*, 1985). These data were corrected for systematic errors by NASA, and were resampled to a pixel resolution of 28.5 m. As shown in Figure 2, the sidelap yields a *B/H* ratio of approximately 0.18 and encompasses a 55–km wide strip of terrain.

A 15–km by 12–km mountainous area located within the sidelap near Tiger, Georgia was selected to test the *LRMS* stereocorrelation algorithms. This study area appears on the U.S. Geological Survey (USGS) 1:24,000–scale Tiger Quadrangle (1957, photorevised 1972) and is characterized by relief to 500 m. It includes a number of well-defined road intersections, bridges, and other features that were used as ground control points (GCPs).

IMAGE RECTIFICATION AND REGISTRATION

Before images can be correlated by automated techniques, they must be rectified to a common coordinate system and placed in precise registration. Two approaches can be considered: (1) parametric and (2) nonparametric.

A parametric approach assumes all imaging parameters at each recording step are known and that all necessary geometric corrections can be reconstructed from the recorded signal and ancillary data. In practice, however, parametric models make use of a subset of the imaging parameters and must consider modeling and mensuration errors. Both the Scrounge and the Thematic Mapper Image Processing System (TIPS) algorithms developed by General Electric derive parametric correction matrices from the satellite payload and mirror scan correction data. They take into account satellite attitude and ephemeris, high frequency structural disturbances, TM sensor characteristics, and desired cartographic projections to produce image data sets of excellent internal geometric integrity (Beyer *et al.*, 1984; Brooks *et al.*, 1984; Beyer, 1985). However, it remains difficult to recover Universal Transverse Mercator (UTM) or geographic (latitude, longitude) coordinates without reference to ground control points.

In order to ensure both images of a stereopair are mapped to a single, standard coordinate system, it is necessary to rectify them to a set of GCPs for which the UTM coordinates have been determined from large scale maps. This is a non-parametric approach in which a mathematical function relating image and ground coordinates is developed and can be used without access to the ancillary data recorded during acquisition. Once this function has been established, it can be applied to fit all pixels to the map coordinate system. Welch *et al.* (1985) have shown

PHOTOGRAMMETRIC ENGINEERING AND REMOTE SENSING,
Vol. 53, No. 9, September 1987, pp. 1231–1237

0099-1112/87/5309–1231$02.25/0

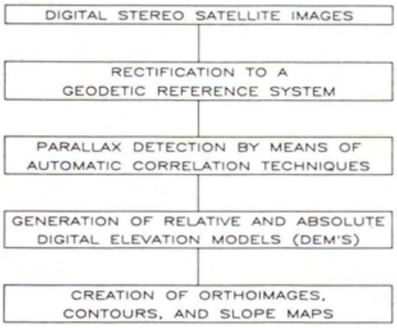

FIG. 1. Steps for the automated generation of map products from digital images

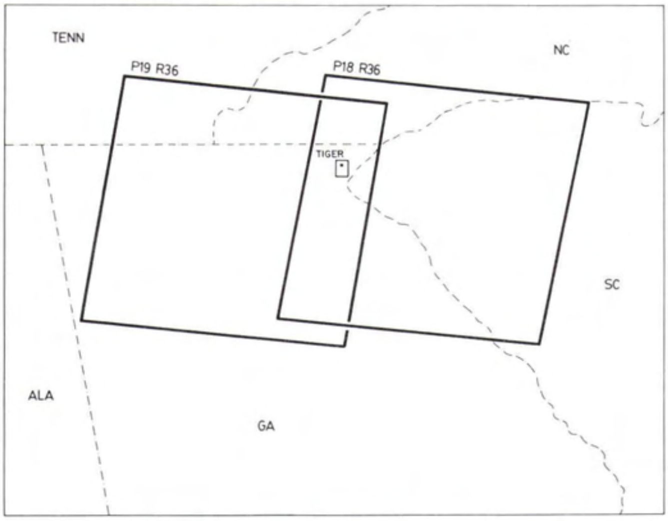

FIG. 2. Location map for Landsat–4 scenes P19R36 (ID E–40153–15404, 12–16–82) and P18R36 (ID E–40144–15335, 11–07–82) showing the sidelap and the test area.

TABLE 1. RECTIFICATION ACCURACY FOR LANDSAT-4 TM IMAGES, P18R36 AND P19R36, TIGER QUADRANGLE. THE ELEVATION OF CONTROL AND CHECK POINTS IS APPROXIMATELY 550 M.

Scene	8 Control Pts. $RMSE_{xy}$	5 Check Pts. $RMSE_{xy}$
P18R36	±20 m	±25 m
P19R36	±22 m	±22 m

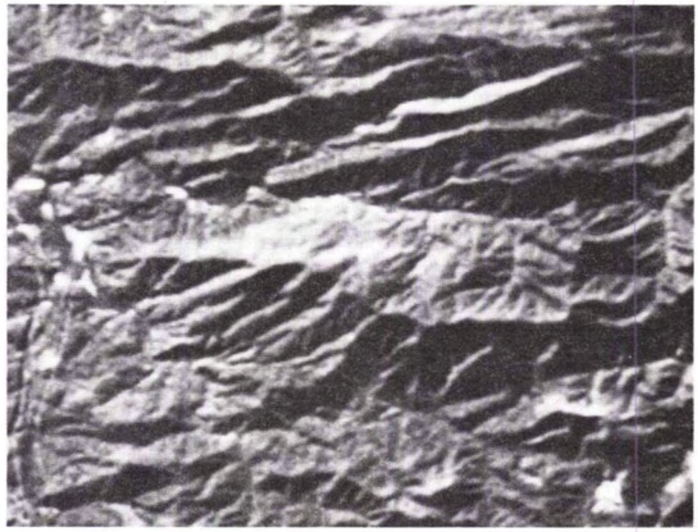

FIG. 3. Band 4 image of a study site subset (7.3 km by 6.8 km). The image has been rectified to the UTM projection. Note: north is toward the bottom of the image.

that TM data can be rectified to a fraction of a pixel using a first degree polynomial equation of the form

$$\mathrm{UTM} = c_0 + c_1x + c_2y \tag{1}$$

where x and y are the pixel and line image coordinates of the GCPs. Coefficients (c) are determined by the method of least squares, and the equations are solved to obtain the easting and northing coordinates in the UTM system.

When rectifying a stereopair of digital images prior to submission to a correlation program, it is desirable to use GCPs that appear in both images and are of approximately uniform elevation. In this instance, 13 GCPs common to both images and within an elevation range of 500 m to 600 m were located in the test data corresponding to the Tiger Quadrangle. Eight points were used for a first degree polynomial rectification, and five points were withheld to evaluate the accuracy of the rectification process. The root-mean-square planimetric error ($RMSE_{xy}$) values of ±22 m to ±25 m for the withheld points are typical of results obtained to-date for data sets of rugged terrain (Table 1).

If rectification can be satisfactorily accomplished, any remaining displacements between the two data sets are assumed to be due to relief (Figure 3). The rectified images may then be assigned to the red and the blue and green guns of the RGB display to create an anaglyph image that can be viewed in stereo.

PARALLAX ESTIMATION TECHNIQUES

If true epipolar geometry existed between images of a stereo pair, it would be possible to utilize fast one-dimensional correlation techniques for parallax detection; however, in practice a slower two-dimensional approach is applied on a pixel-by-pixel basis to accomodate variabilities, residual geometric distortions, and radiometric noise in the image data. With the Landsat TM's field-of-view of about 15 degrees, parallaxes of as much as four pixels can be expected for terrain relief of 500 m. Thus, to produce Z-coordinates compatible with mapping requirements, refined correlation and interpolation procedures yielding subpixel accuracies are necessary.

As illustrated in Figure 4, each image pixel in the reference image (1) of the stereopair represents the center of a correlation window of N_1 lines by M_1 columns. Because the stereo images (1) and (2) have been rectified and then placed in register, the search window in the search image (2) with N_2 lines by M_2 columns ($N_1<N_2, N_1<M_2$) has the same center coordinates as the corresponding correlation window. By moving the correlation window over all possible locations within the search window, a matching function determines the point of maximum similarity. The parallax is determined by the difference in coordinates for this matching location and that of the original pixel in the reference image.

Various mathematical functions have been proposed for the actual matching process (Barnea and Silverman, 1972; Dowman and Haggag, 1977; Horn, 1983; Foerstner, 1984; Ehlers, 1985). In practice, the highest precision has been obtained with least-squares based models which are equivalent to maximizing the product moment correlation coefficient of the signals (Ackermann, 1984; Mikhail *et al.*, 1984). Consequently, the "normal" product moment correlation function $c\,(\triangle x,\triangle y)$ has been employed as an objective function for the matching process of the two image signals s_1 and s_2: i.e.,

$$c(\triangle x,\triangle y) = \int_{-\infty}^{\infty}\int_{-\infty}^{\infty} s_1\,(x,y)\cdot s_2(x+\triangle x, y+\triangle y)dxdy \tag{2}$$

Reliability of the correlation may be improved by selecting a variance threshold for the correlation window to avoid corre-

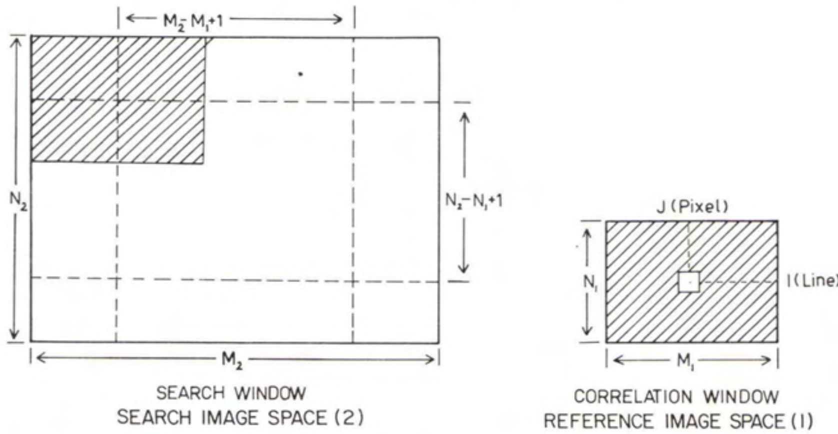

FIG. 4. Two-dimensional matching principle. The correlation window ($N_1 \times M_1$) is moved over all possible locations within the search window ($N_2 \times M_2$). At each location, the correlation coefficient is computed.

lation in low contrast areas which can lead to serious mismatches (Ehlers, 1982). The window sizes for the correlation and search windows can be adjusted according to image content and signal-to-noise ratio (SNR).

The procedure works in an iterative manner starting with a large correlation window. In successive stages, correlation is performed with smaller windows around the point indentified in the preceding step. At the last iteration, a two- or one-dimensional polynomial of second degree is fitted to the 3 by 3 or 3 by 1 correlation values around the computed maximum. The maximum value of the interpolating polynomial function redefines the coordinates of the matching point to subpixel accuracy.

Correlations were performed with data from spectral band 4 which is reported to have the highest SNR (Irons, 1985). The correlation between reference and search images was carried out in two steps. At the first step, correlation was achieved by moving an 11 by 11 correlation window within a 21 by 13 search window, allowing ± 1 pixel maximum deviation in the y-direction (along track) and ± 5 pixel in the x-direction (cross track). These values for the correlation and search windows were based on the accuracy of the rectification, the existing relief in the study area, and the maximum parallax likely to be encountered. In the second step, the points of maximum correlation were refined by moving a 5 by 5 window inside a 7 by 7 search window. This 5 by 5 window represents an approximate 140–m by 140–m square area on the ground, therefore acting as a low pass filter. Once the pixel location of maximum signal was determined, a polynomial interpolation established the point of correlation to subpixel accuracy. This procedure was iterated on a per-pixel basis to produce terrain coordinates for each data point.

From initial tests at sample points in the image, a minimum variance value of 10.0 was estimated as the threshold for reliable correlation. With this threshold, 4.7 percent of the image pixels could not be processed and the parallax values for these points were interpolated as weighted averages from their successfully correlated neighbors. To correct for single outliers, the parallax file was filtered with a one-dimensional filter mask $F = (1,1,0,1,1)^T$ and an appropriate threshold value. The computed parallax differences for a screen-sized subarea are displayed as 8-bit data in Figure 5.

DIGITAL ELEVATION MODEL (DEM) COMPUTATION

A *relative* DEM can be generated from the computed parallaxes. For cross-track stereo such as is the case with Landsat and SPOT, the relative height (dh) at each image point (x,y) is a function of the differential parallax (dx), the altitude (H) of the satellite and the distance (B) between the adjacent orbits. Thus,

$$dh\ (x,y) = dx\ (x,y) \quad H/B$$

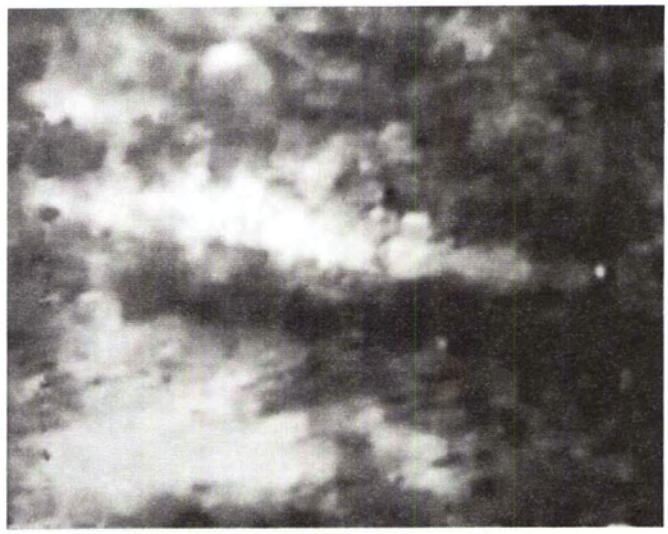

FIG. 5. 8–bit display of the parallaxes obtained from stereo correlation of the Landsat TM images. Maximum parallaxes are displayed as white, minimum parallaxes as black.

This well-known equation can be slightly modified if the satellite orbits are not exactly parallel and there is a discrepancy in the orientation of the scan lines as a function of the line number y: i.e.,

$$dh\ (x,y) = dx\ (x,y) * H/B(y). \tag{4}$$

$B(y)$ is computed as a linear interpolation function if the stereo base is known at two or more image locations in the along-track direction. For the Landsat TM subsets employed in this study (H = 705 km; $B \sim$ 130 km), the variation in B/H ratio is less than 0.004 and the satellite tracks are assumed to be parallel with a B/H ratio of 0.18.

The relative DEM values may be scaled by linear least-squares techniques to GCPs of known Z-coordinates to obtain terrain elevations for each pixel, thus creating an *absolute* DEM. In this instance, an absolute DEM for the digital TM data (TM DEM) was computed for the 527– by 422–pixel matrix of the study area by scaling the dh values for each of the pixels to fourteen GCPs at known elevations ranging between 480 and 920 m. The accuracy of the TM DEM was checked by three methods: (1) analysis of Z-errors at withheld check points; (2) comparison of contour lines derived from the TM DEM with contours interpolated from the reference map and from an existing USGS DEM (Figure 6; and (3) pixel-by-pixel comparison of the TM and USGS DEMs.

FIG. 6. 8–bit display of the USGS DEM. Elevations are represented by light (high) to dark (low) gray values.

Z-ERRORS AT INDEPENDENT CHECK POINTS

The Z-errors at seven withheld check points ranging in elevation from 480 to 870 m yielded an $RMSE_z$ value of ± 42 m (Figure 7). This value corresponds to a planimetric correlation error of about ± 0.3 pixel, confirming the much discussed feasibility of achieving correlation to better than ± 0.5 pixel.

If the errors in the Z-coordinates are defined as an $RMSE_z$ value, the well-known relationship of 3.3·$RMSE_z$ yields the closest contour interval (CI) likely to meet U.S. National Map Accuracy Standards (NMAS). Thus, for an $RMSE_z$ value of ± 42 m, a contour interval of between 100 m and 150 m is indicated.

COMPARISON OF CONTOUR LINES AND ELEVATIONS

A set of 100–m reference contours was interpolated from the 20-ft contours depicted on the 1:24,000–scale Tiger sheet (Figure 8a). These interpolated reference contours are estimated to have an error of ± 2 to ± 3 m (in Z) at the one-sigma level of confidence.

A corresponding set of 100–m contours were developed from the USGS DEM for the Tiger sheet. This was accomplished by registering the DEM to the Landsat TM image data set and resampling to transform the 30–m pixels to 28.5-m pixel dimensions (see Figure 6). Contours were then generated by applying a density slicing technique to the resampled DEM so that pixels at 100–m intervals were displayed to form the contours (Figure 8b). The USGS DEM has an $RMSE_z$ value of only ± 8.8 m (Usery, 1985). Consequently, contours interpolated at a 100–m interval from the USGS DEM should have negligible errors in planimetric position.

Contours at a 100–m interval were then produced from the TM stereo data (Figure 8c). This was accomplished by using the same density slicing technique previously applied to the USGS DEM. The excellent correspondence of contours developed from the USGS and TM DEMs is shown in Figure 9.

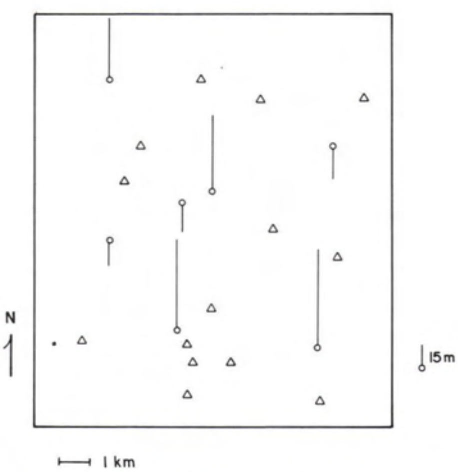

FIG. 7. Distribution of control points (triangles) and check points (circles) used for DEM calibration and checking. $RMSE_Z$ values are shown for the check points only.

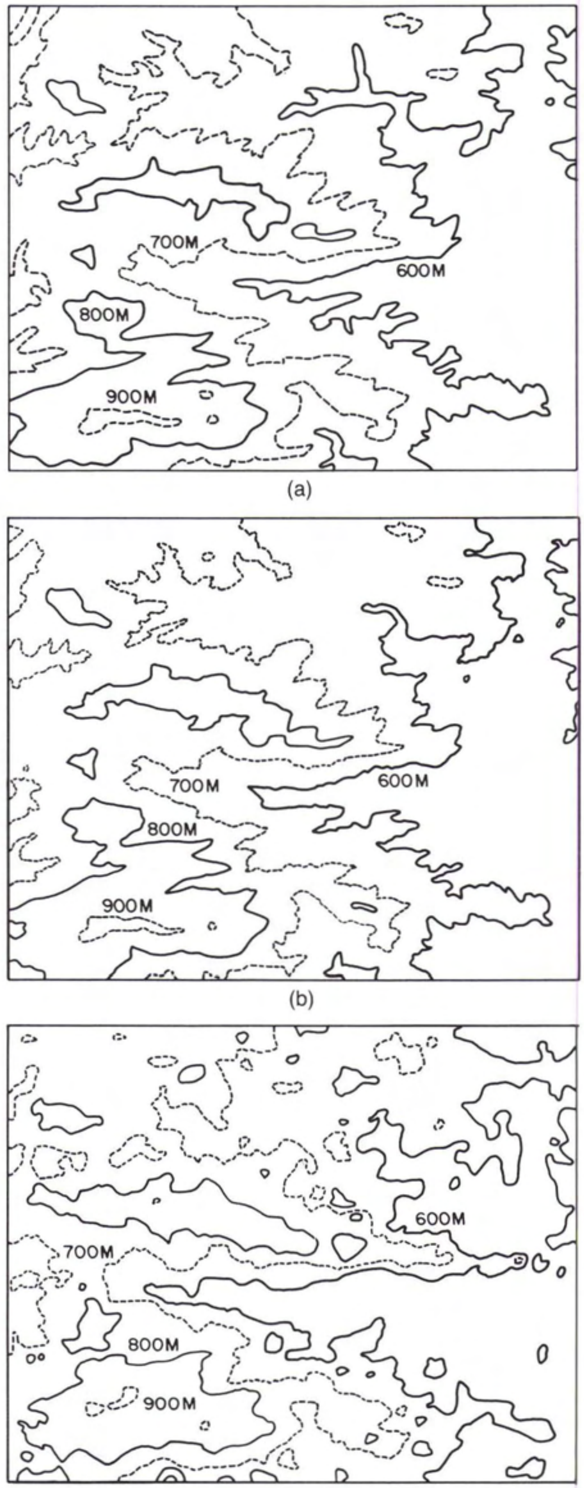

FIG. . Contours (100–m interval) interpolated from the (a) 1:24,000 USGS topographic map (b) USGS DEM and (c) TM DEM.

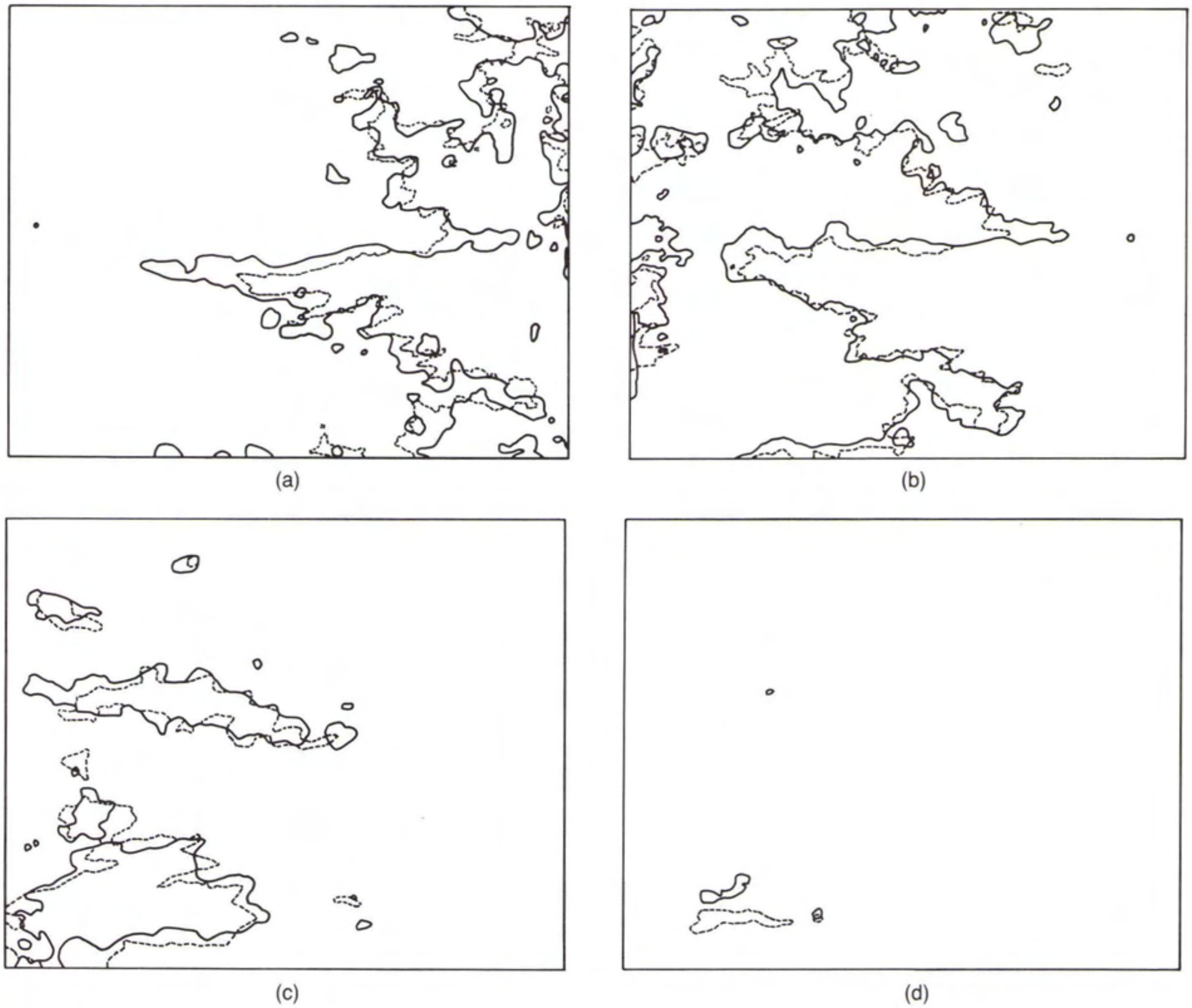

FIG. 9. Single contours from the TM DEM (solid lines) and the USGS DEM (dashed lines) for (a) 600–m (b) 700–m (c) 800–m (d) 900–m elevation.

In addition, the above contours were compared against the 100–m reference contours from the 1:24,000–scale Tiger map sheet. The elevation of random sample points along the TM and USGS DEM contours were interpolated from the adjacent 100–m reference contours as shown in Figure 10 to yield $RMSE_z$ values of ± 33 m and ± 12 m, respectively.

As a further assessment of accuracy, the differences in elevation at corresponding pixel locations for the TM and USGS DEMs were determined by subtracting the two DEMs. The histogram of these differences yielded a mean value of 5.5m and a standard deviation of 39.0 m (Figure 11).

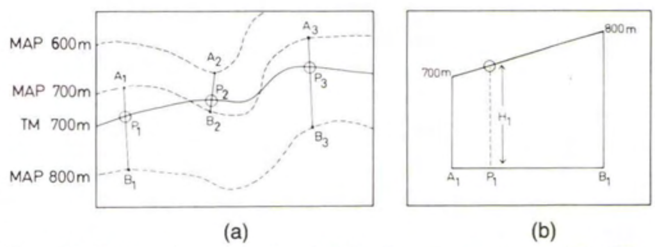

FIG. 10. Contour line accuracy test for the TM and USGS DEMs. For random test points P_i along the TM and USGS DEM contours, (a) the minimum distance to the adjacent map contours is determined and (b) the height at each P_i is computed by linear interpolation.

DIGITAL MAP PRODUCTS FROM SATELLITE IMAGE DATA

Image data in digital formats can be used to create orthoimages, topographic maps, and perspective views of the terrain by automated procedures (Faintich, 1985; Ehlers and Welch, 1985; Dubayah and Dozier, 1986) (Figure 12). For example, government agencies, including the U.S. Geological Survey and France's Institut Geographic National (IGN), and industries such as MacDonald Dettwiler are already convinced that high resolution satellite image data in digital formats will prove suitable for producing maps at scales of 1:50,000 and smaller (Colvocoresses, 1986; Rose *et al.*, 1986; Baudoin, 1986).

In order to meet this objective, however, it will be necessary to generate DEMs at accuracies compatible with recognized standards for vertical accuracy, e.g., 68 percent of the DEM grid elevations should be correct to within one-third the contour interval. Factors influencing the accuracy of elevations include residual geometric errors in the data after rectification and the heighting precision obtained during the correlation process. In Figure 13, for example, estimated $RMSE_z$ values are plotted as a function of B/H ratio for satellite data having pixel resolutions of 10, 20, and 30 m. The curves are based on an overall planimetric measurement or correlation error of ± 0.75 pixel. With a B/H ratio of 1.0 and a 10–m pixel resolution, typical of SPOT–1 panchromatic data, $RMSE_z$ values of better than ± 10 m can be expected (Welch, 1985).

A major bottleneck in the preparation of maps from satellite data, however, is the computational requirement for pixelwise stereo processing. For a two-step iteration process with subpixel interpolation and variance pre-checking, the current LRMS procedures encompass more than 50,000 arithmetic operations per

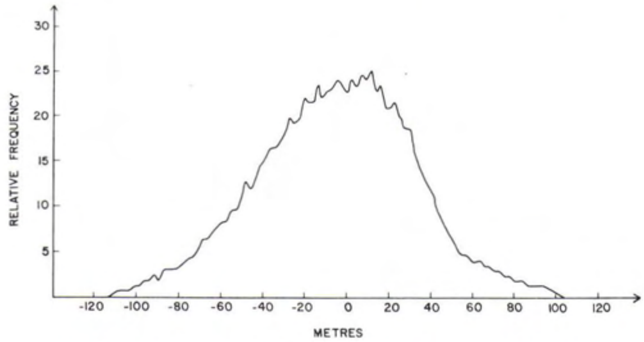

FIG. 11. The histogram of elevation differences between the USGS DEM and the TM DEM yielded a mean error of 5.5 m and a standard deviation of 39.0 m.

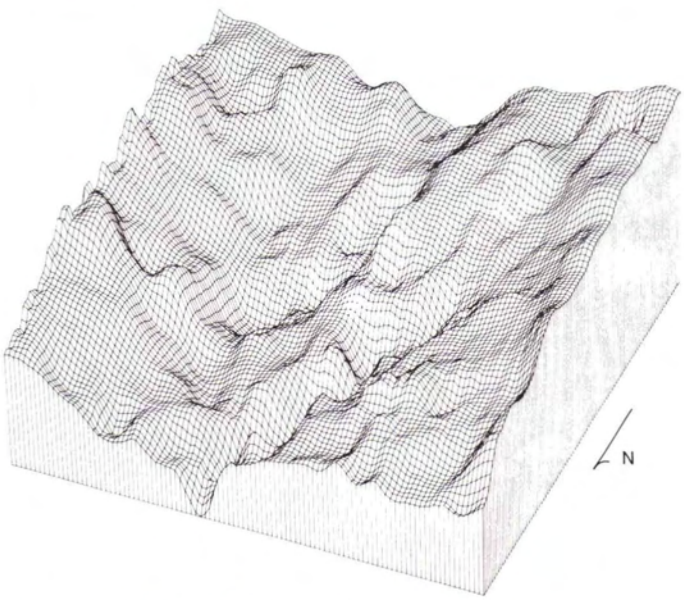

FIG. 12. Perspective view for a 100 by 100 pixels subset of the TM DEM.

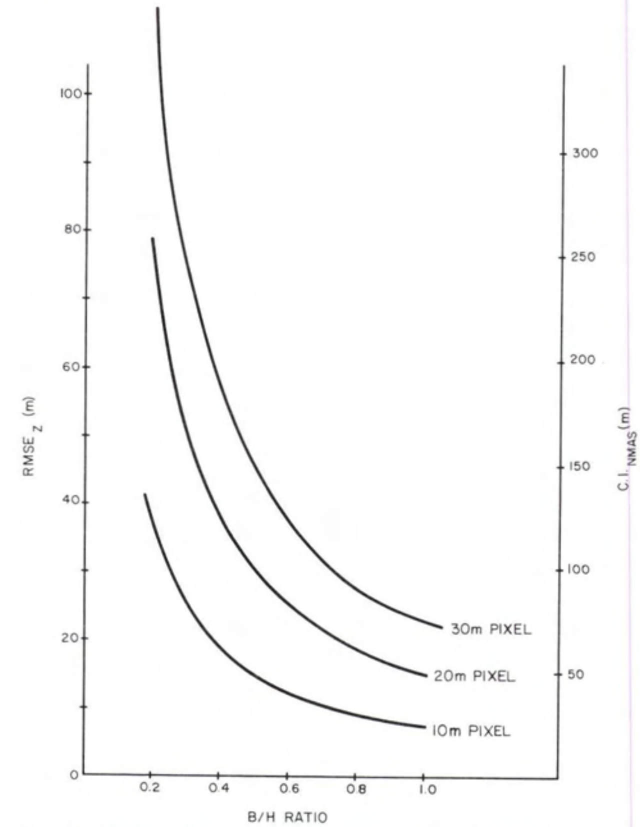

FIG. 13. $RMSE_Z$ value and closest NMAS contour interval (CI_{nmas}) in metres versus base-to-height ratio for spatial data resolutions of 10 m, 20 m, and 30 m. An absolute measurement (correlation) error of ± 0.75 pixel is assumed.

pixel. On a dedicated minicomputer the computational time will range between 0.2 and 10 seconds per pixel. It should be noted that a single SPOT HRV scene covering 60 km by 60 km at 10–m resolution contains approximately 36,000,000 pixels. Consequently, to reduce computation time, consideration must be given to advanced techniques involving parallel processing on single-instruction, multiple-data (SIMD) and multiple-instruction, multiple-data (MIMD) computer systems (Panton, 1978; Fischel, 1983; Ozga, 1984; Tilton and Strong, 1984; Ramapriyan *et al.*, 1986).

Studies are currently underway to implement the LRMS stereocorrelation software on the University of Georgia's Control Data Corporation (CDC) CYBER 205 and CYBERPLUS supercomputer systems. Experience to-date indicates that the computation time per point can be reduced to milliseconds on the CYBER 205 SIMD system.

CONCLUSION

Digital elevation models can be derived from stereo satellite image data of high resolution by automated correlation techniques. In this study, an $RMSE_z$ value of $\pm$ 42 m was achieved for a DEM developed from sidelapping Landsat–4 TM scenes. Comparison of 100–m contours generated by automated techniques with reference contours traced from an existing USGS 1:24,000-scale quadrangle revealed a *Z*-error of approximately ± 33 m. Thus, the DEM is of sufficient accuracy for the production of orthoimages and perspective image products, or for the interpolation of contours for small-scale topographic maps.

It is anticipated that satellite images of 10–m or 20–m pixel size and *B/H* ratios of 0.6 to 1.0 from the SPOT–1 and future satellite programs will permit $RMSE_z$ values to be reduced to less than ± 10 m, thus allowing vertical accuracy standards compatible with topographic maps of 1:25,000 and smaller to be realized. However, the processing constraints imposed by the tremendous amount of data and by computational intensive tasks such as stereocorrelation are subjects that must be addressed.

The possibilities for DEM generation from large stereo data sets are currently limited by the computer configurations commonly employed for image processing and mapping tasks. Consequently, developments in parallel or distributed processing are likely to be required to facilitate automated, three-dimensional mapping from digital satellite imagery.

ACKNOWLEDGMENT

Support for this work was provided by the National Aeronautics and Space Administration (NASA) under contract NAS5-27383 and by the Deutsche Forschungsgemeinschaft (DFG) under the research stipend Eh 85/1–1.

REFERENCES

Ackermann, F., 1984. Digital Image Correlation: Performance and Potential Application in Photogrammetry. *Photogrammetric Record*, 11 (64), pp. 429–439.

Barnea, D.I., and H.F. Silverman, 1972. A Class of Algorithms for Fast Digital Image Registration. *IEEE Trans. Computer*, Vol. C–21, pp. 179–186.

Baudoin, A., 1986. Preliminary Results from SPOT 1. *Proceedings of the ISPRS Commission IV Symposium*, Edinburgh, Scotland, IAPRS XXVI–4, p. 1.

Bernstein, R., 1976. Digital Image Processing of Earth Observation Sensor Data. *IBM Journal of Research and Development*, Vol. 20, pp. 40–57.

Beyer, E.P., 1985. An Overview of the Thematic Mapper Geometric Correction System. *Landsat–4 Science Characterization: Early Results*, NASA Conference Publication 2355, Vol. II, pp. II–87 to II–145.

Beyer, E.P., J. Brooks, and V.V. Salomonson, 1984. Geometric Correction of Landsat 4 and 5 Thematic Mapper Data. *Proceedings of the XVIIIth International Symposium on Remote Sensing of Environment*, Paris, France, pp. 89–100.

Borgeson, W.T., R.M. Batson, and H.H. Kieffer, 1985. Geometric Accuracy of Landsat–4 and Landsat–5 Thematic Mapper Images. *Photogrammetric Engineering and Remote Sensing*, Vol. 51, No. 12, pp. 1893–1898.

Brooks, J., A. Jai, T. Keller, E. Kimmer, and J. Su, 1984. Thematic Mapper Geometric Correction Performance Evaluation. *Proceedings of the 10th International Symposium on Machine Processing of Remotely Sensed Data*, Purdue University, West Lafayette, Indiana, pp. 22–28.

Colvocoresses, A.P., 1982. An Automated Mapping Satellite System (MAPSAT). *Photogrammetric Engineering and Remote Sensing*, Vol. 48, No. 10, pp. 1585–1591.

———, , 1986. Image Mapping with the Thematic Mapper. *Photogrammetric Engineering and Remote Sensing*, Vol. 52, No. 9, pp. 1499–1505.

Dowman, I.J., and A. Haggag, 1977. Digital Image Correlation Along Epipolar Lines. *Mitteilungen der Geodaetischen Institute der TU Graz*, Vol. 29, pp. 47–49.

Dubayah, R.O., and J. Dozier, 1986. Orthographic Terrain Views Using Data Derived from Digital Elevation Models. *Photogrammetric Engineering and Remote Sensing*, Vol. 52, No. 4, pp. 509–518.

Ehlers, M., 1982. Increase in Correlation Accuracy by Digital Filtering. *Photogrammetric Engineering and Remote Sensing*, Vol. 48, No. 3, pp. 415–420.

———, , 1985. The Effects of Image Noise on Digital Correlation Probability. *Photogrammetric Engineering and Remote Sensing*, Vol. 51, No. 3, pp. 357–365.

Ehlers, M., and R. Welch, 1985. Satellite Remote Sensing Data as Input to Geographic Information Systems. *Proceedings of the 11th International Symposium on Machine Processing of Remotely Sensed Data*, Purdue University, West Lafayette, Indiana, p. 219.

Faintich, M.B., 1985. Defense Mapping Undergoes a Digital Revolution. *Computer Graphics World*, June 1985, pp. 10–28.

Fischel, D., 1983. Some Current Uses of Array Processors for Preprocessing of Remote Sensing Data. *Proceedings of the XVIIth International Symposium on Remote Sensing of Environment*, Ann Arbor, Michigan, Vol. 1, pp. 186–195.

Foerstner, W., 1984. Quality Assessment of Object Location and Point Transfer Using Digital Image Correlation Techniques. *Invited Paper, Proceedings of the XVth International Congress of ISPRS*, Rio de Janeiro, Brazil, IAPRS XXV/A3a, pp. 197–219.

Horn, B.K.P., 1983. Non-Correlation Methods for Stereo Matching. *Photogrammetric Engineering and Remote Sensing*, Vol. 49, No. 4, pp. 535–536.

Irons, J.R., 1985. An Overview of Landsat-4 and the Thematic Mapper. *Landsat-4 Science Characterization: Early Results*, NASA Conference Publication 2355, Vol. II, pp. II–15 to II–46.

Mikhail, E.M., M.L. Akey, and O.R. Mitchell, 1984. Detection and Sub-Pixel Location of Photogrammetric Targets in Digital Images. *Photogrammetria*, Vol. 39, pp. 63–83.

Murai, S., and R. Shibasaki, 1984. A Study of Three Dimensional Measurement with Use of Stereo Linear Array Sensor. *Proceedings of the XVth International Congress of ISPRS*, Rio de Janeiro, Brazil, IAPRS XXV-A3b, pp. 759-767.

Ozga, M., 1984. Experience with the Use of Supercomputers to Process Landsat Data. *Proceedings of the 10th International Symposium on Machine Processing of Remotely Sensed Data*, Purdue University, West Lafayette, Indiana, pp. 276–280.

Panton, D.J., 1978. A Flexible Approach to Digital Stereo Mapping. *Photogrammetric Engineering and Remote Sensing*, Vol. 45, No. 12 , pp. 1499–1512.

Ramapriyan, H.K., J.P. Strong, Y. Hung, and C.W. Murray, 1986. Automated Matching of Pairs of SIR-B Images for Elevation Mapping. *IEEE Transactions on Geosciences and Remote Sensing*, Vol. GE–24, No. 4, pp. 462–472.

Rose, D.R., I. Laverty, and M. Sondheim, 1986. Base Map Production from Geocoded Imagery. *Proceedings of the ISPRS Commission VII Symposium*, Enschede, The Netherlands, IAPRS XXVI–7/1, pp. 67-71.

Rosenholm, D., 1986. Accuracy Improvement of Digital Matching for Evaluation of Digital Terrain Models. *Proceedings of the ISPRS Commission III Symposium*, Rovaniemi, Finland, IAPRS XXVI–3/2, pp. 573–587.

Simard, R., and V.G. Krishna, 1983. A Successful Approach in Three-Dimensional Perception of Stereo Landsat-MSS Images over Cordilleran Relief. *Proceedings of the 9th International Symposium on Machine Processing of Remotely Sensed Data*, West Lafayette, Indiana, pp. 31–40.

Simard, R., R. Oliver, and E. Pina, 1984. Digital Elevation Modeling with Landsat-3 RBV Data. *Proceedings of the XVIIIth International Symposium on Remote Sensing of Environment*, Paris, France, pp. 825–834.

Tilton, J.C., and J.P. Strong, 1984. Analyzing Remotely Sensed Data on the Massively Parallel Processor. *Proceedings of the 10th International Symposium on Machine Processing of Remotely Sensed Data*, Purdue University; West Lafayette, Indiana, pp. 281–288.

Usery, E.L., 1985. *A Raster Database Approach to Topographic Map Revision*. Ph.D. Thesis, University of Georgia, 326 p.

Welch, R., 1983. Impact of Geometry on Height Measurements from MLA Digital Image Data. *Photogrammetric Engineering and Remote Sensing*, Vol. 49. No. 10, pp. 1437–1441.

———, , 1985. Cartographic Potential of SPOT Image Data. *Photogrammetric Engineering and Remote Sensing*, Vol. 51. No. 8, pp. 1085–1091.

Welch, R., and W. Marko, 1981. Cartographic Potential of a Spacecraft Line Array Camera System: Stereosat. *Photogrammetric Engineering and Remote Sensing*, Vol. 47, No. 8, pp. 1173–1185.

Welch, R., and E.L. Usery, 1984. Cartographic Accuracy of LANDSAT-4 MSS and TM Data. *IEEE Transactions on Geoscience and Remote Sensing*, Vol. GE–22, No. 3, pp. 281–288.

Welch, R., and M. Ehlers, 1985. Digital Image Processing Techniques for Deriving Terrain Coordinates from Satellite Image Data. *Technical Papers, 51st Annual Meeting ASP*, Washington, D.C., Vol. 2, p. 875.

Welch, R., T.R. Jordan, and M. Ehlers, 1985. Comparative Evaluations of the Geodetic Accuracy and Cartographic Potential of Landsat-4/-5 TM Image Data. *Photogrammetric Engineering and Remote Sensing*. Vol. 51, No. 9, pp. 1249–1262.

Wong, K.W., 1975. Geometric and Cartographic Accuracy of ERTS–1 Imagery. *Photogrammetric Engineering*, Vol. 41, No.5 pp. 612–635.